

ULTRA WIDEBAND SAS IMAGING

Stig Asle Vaksvik Synnes^a, Roy Edgar Hansen^a

^aNorwegian Defence Research Establishment, PO Box 25 – N 2027 Kjeller, Norway

Contact author: Stig Asle Vaksvik Synnes, Norwegian Defence Research Establishment, PO Box 25 – N 2027 Kjeller, Norway, e-mail: Stig-Asle.Synnes@ffi.no, fax: +47 63807509.

Abstract: *In synthetic aperture sonar (SAS) processing we coherently combine data from multiple pings in order to synthesize an aperture that is significantly longer than the physical array. The resulting images have a high along-track resolution that is independent of range and frequency. We believe that concurrent high resolution imaging at high frequencies (HF) and low frequencies (LF) will significantly improve the target classification ability. However, for successful SAS processing on ultra wideband low frequency signals, several challenges must be met.*

In October 2012, the NATO Centre for Maritime Research and Experimentation (CMRE) facilitated the ARISE'12 trials from the research vessel Alliance, off of Elba island, Italy. During this trial, the Norwegian Defence Research Establishment (FFI) recorded concurrent HF and LF data using the HISAS1030 SAS with added prototype LF-capability on a HUGIN autonomous underwater vehicle (AUV). The HF and LF bands studied here have a bandwidth of 25 kHz, centred on 72.5 kHz and 25 kHz.

In this article we compare different SAS image processing schemes for ultra wideband signals. We suggest a processing scheme adopting the best features from both time domain back projection (TDBP) and wavenumber domain (WD) imaging; the general track from TDBP and the wavenumber filtering from WD. The performance of the different processing schemes is validated through both simulations and measurements.

Keywords: *Synthetic Aperture Sonar, Ultra Wideband, Widebeam, Low Frequency Imaging*

1. INTRODUCTION

We investigate synthetic aperture sonar (SAS) ultra wideband (UWB) imaging using a 12-38 kHz chirp signal. The sonar system consists of a HISAS1030 SAS with a prototype low frequency (LF) transmitter add-on on a HUGIN autonomous underwater vehicle (AUV), shown in Fig. 1. The UWB-LF data can be recorded alone or concurrently with a high frequency (HF) band of 25 kHz bandwidth centred on 72.5 kHz. For concurrent recording, the range is reduced by a factor two, in order not to increase the data rate.



Fig. 1: Norwegian Defence Research Establishment's HUGIN AUV equipped with a HISAS 1030 SAS system (60-115 kHz) and an added prototype low frequency transmitter (12-38 kHz)

The main advantage of SAS imaging is range-independent high resolution imagery with a large area coverage rate. Its applications comprise areas such as military and civilian mapping and recognisance, underwater archaeology, pipeline inspection and mine hunting.

Low frequency sonar systems have the potential of penetrating into both sediment and objects. Wideband and dual band SAS systems also can reveal the frequency dependency of the acoustic scattering, and thereby indicate the physical properties of the scene. Multi-chromatic anomaly detection has been used with success on optical hyperspectral images, and is also a candidate to operate directly on high-resolution multi-band sonar images. Research has also been done into identification by comparing LF angular-frequency response of image to those of known targets.[1]

In this paper we consider how to obtain good LF SAS image formation by adapting the HF SAS processing scheme.

2. WIDEBAND VERSUS NARROWBAND SAS

In synthetic aperture sonar processing we coherently combine data from multiple pings in order to synthesize an aperture that is significantly longer than the physical array. To a first order (narrowband) approximation the range resolution is given by the signal bandwidth (to give $\delta_r = c/2B$) and the along track resolution by the angular wavenumber coverage (to give $\delta_x = d/2$).[2]

The maximum along track resolution is half that of the element size, d , and results from combining the signals from all pings ensonifying the scene. With a fixed element size the narrowbeam approximation of the 3dB beamwidth is $\beta = \lambda/d$, where λ is the wavelength. The required aperture length therefore rapidly increases with decreasing frequency. The resulting aperture length is illustrated for HF- and LF-bands in Fig. 2.

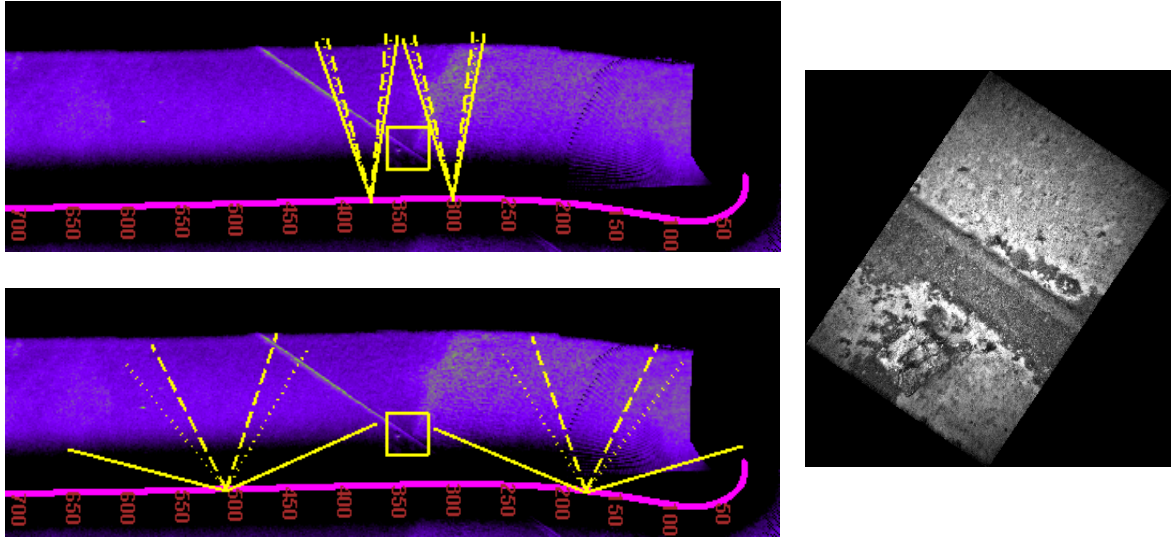


Fig. 2: Left: A 20 m x 20 m area for later SAS imaging, here indicated in HF sidescan images. The 3dB beamwidth and required ping interval is shown for our HF band at the top and for our LF band at the bottom. The HF band spans 60-85 kHz, and the LF band spans 12-38 kHz. The different lines address the lowest (-), centre (...) and highest (--) frequency of each band. Right: Optical details of the SAS imaging scene, showing a pipeline and a concrete cube.

There are two main methods of SAS image formation: Time Domain Back Projection (TDBP) and Wavenumber Domain (WD) imaging. In TDBP the recorded time series are back propagated to each pixel of the scene. In WD the time series are converted into the frequency domain and added to the image spectrum applying the Stolt migration. For the case of narrowband and narrowbeam, the major difference has been that the WD method is much faster, though the TDBP method is slightly more robust to track nonlinearities.[3][4]

For a wideband and low frequency case, with around 90 degrees 3dB beamwidth, several synthetic aperture processing issues arise.[5] Both of the above mentioned methods are expected to have reduced performance; the WD method because the track linearity limitation are more difficult to circumvent with this wide beams, and the TDBP method because an optimal ping selection cannot be chosen for the beamwidth of more than one of the involved frequencies (c.f. Fig. 2).

We suggest a wideband processing scheme adopting the best features of both methods, i.e. the general track from TDBP and the wavenumber filtering from WD. The processing speed is not really an issue with fast computers and access to running code on graphical processing units (GPU). We will use TDBP as a starting point and compare the traditional narrowband processing with a multiband processing scheme and our wideband processing scheme. In the remaining of this article, we address each of these methods and illustrate their performance on both a simulation and measurements.

3. SAS IMAGING SCHEMES

The application of TDBP is based on the narrowband assumption that the required angular coverage (or ping interval) is the same for all involved frequencies. The number of pings to be included is then chosen according to the angular coverage required for the desired resolution, and a tapering is applied on the pings to reduce edge effects. This narrowband assumption is valid for the HF band, but that not for the LF band, as illustrated by the frequency dependency of the angular coverage in Fig. 2.

In this chapter we use the wavenumber coverage to consider the applicability to UWB LF signals of the narrowband method, a multiband approach to wideband signals, and our dedicated wideband method. Along with the wavenumber coverage, we also plot the theoretical 3 dB coverage after applying a Kaiser tapering on the range axis and a Hamming window within a processing beamwidth of 3/4 on the along track axis is indicated by red lines. The lines should correspond to the theoretical resolution of the resulting image of $\delta_x = 2\pi/k_x$. However, this depends on the same wavenumber coverage on all frequencies, rounding off smoothly beyond the 3 dB lines.

The resulting images on both simulation and measurements follow in chapter 4.

3.1. Narrowband

The ping interval required to meet a specified along track resolution, is frequency dependent. If the ping interval is chosen based on the highest frequency, only valid data is included for all frequencies, though not all the valid data for the lower frequencies. This would result in a reduced azimuth resolution. If the ping interval is chosen based on the lowest frequency, all the valid data is included, but also excess echoes that is not related to the scene for the higher frequencies. This will result in an addition of aliased energy in to the image in the image and loss of contrast. Choosing the ping interval corresponding to the centre frequency of band could be a reasonable trade off between resolution and signal to noise ratio [6]. Here we choose this latter option, and the resulting wavenumber coverage is shown in Fig. 3.

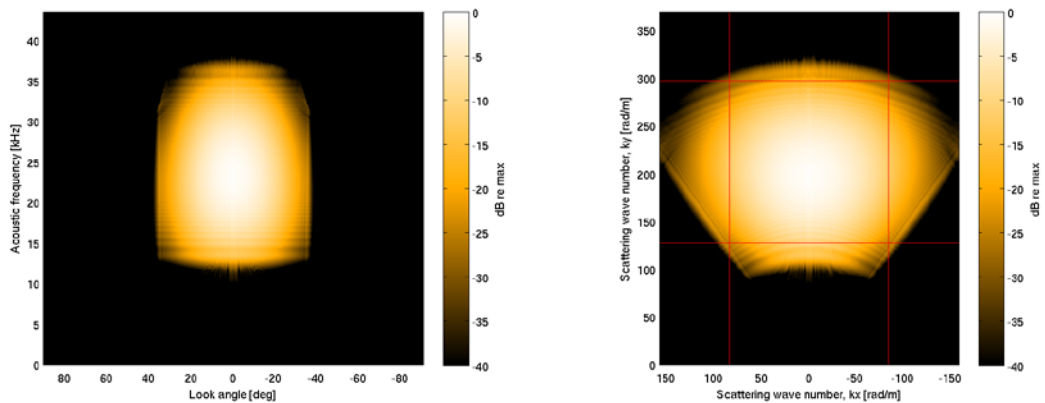


Fig. 3: Narrowband processing on simulated data from a single point scatterer: Angle-frequency coverage (left) and scattering wavenumber (right)

3.2. Multiband

Because the narrowband processing performs better with decreasing bandwidth, a candidate processing scheme is therefore to split the total band into subbands before applying the narrowband processing on each band, as suggested in e.g. [6][7]. This reduces the effect of added noise and degraded resolution. The resulting wavenumber coverage is shown in Fig. 4.

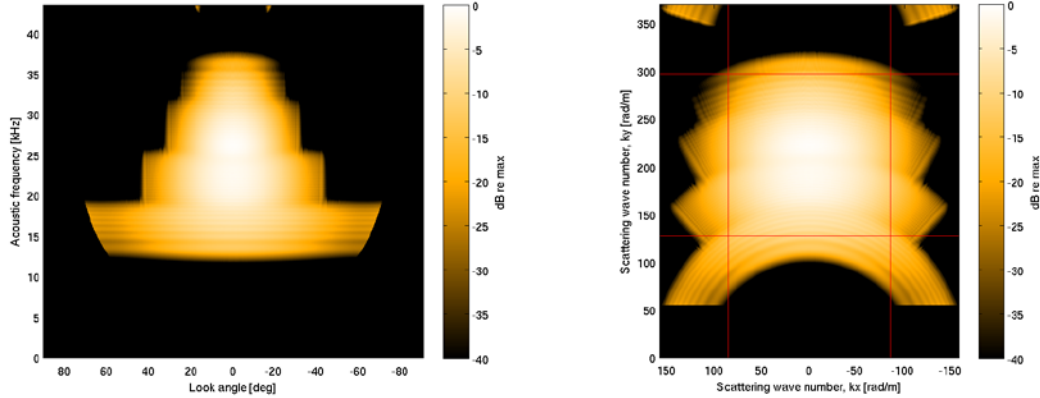


Fig. 4: Multiband processing on simulated data from a single point scatterer: Angle-frequency coverage (left) and scattering wavenumber (right)

3.3. Wideband

Ideally UWB LF imaging should apply the same maximum along track wavenumber coverage for all frequencies, rather than processing a fixed interval of pings for all frequencies or a group of frequencies. One solution would be to process each frequency independently, as in WD processing.

Here we suggest another two-step approach based on both TDBP and WD imaging:

1. Choose the angular coverage of TDBP based on the lowest frequency. This includes all the valid data, but also excess echoes in the higher frequencies that is not related to the scene. The image must be processed on a higher resolution grid in order to assure that the excess frequencies do not fold onto the image information.
2. Apply windowing in wavenumber domain in order to select the desired data coverage for all frequencies. Then down-sample the image to the desired resolution.

With this approach, we obtain full data coverage also for UWB LF signals, taking benefit of the advantages of both the TDBP and the WD method. The extra cost versus the narrowband approach is the higher resolution required and the extra filtering step. The resulting wavenumber coverage is shown in Fig. 5.

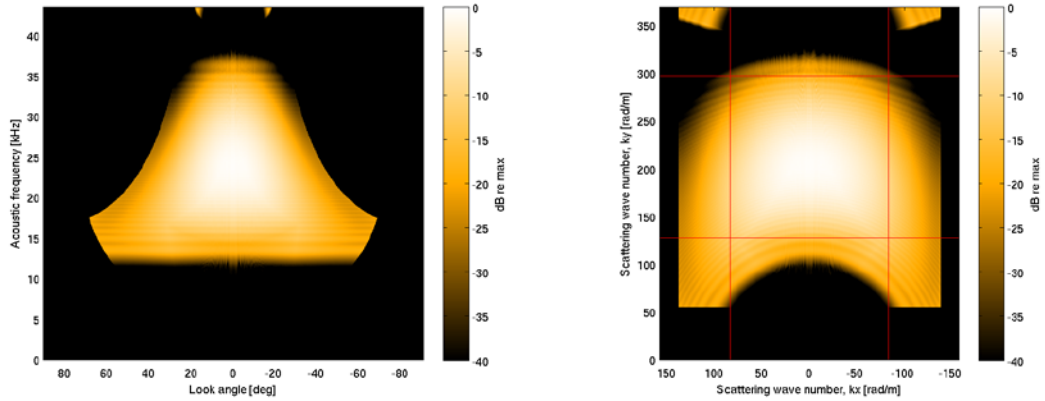


Fig. 5: Wideband processing on simulated data from a single point scatterer: Angle-frequency coverage (left) and scattering wavenumber (right)

4. RESULTS AND DISCUSSION

In Fig. 3, Fig. 4 and Fig. 5, the wavenumber coverage was shown for each of the imaging schemes applied on the LF band. In Fig. 6 we show the corresponding point spread functions.

In Fig. 7 we show an example image of the three processing schemes applied on both HF and LF bands of the real scene depicted in Fig. 1. We observe that in the LF band the details on the cube in particular are sharpest in the wideband processed image, slightly defocused in the multiband processed image and quite blurred in the narrowband processed image. In the HF band, only the multiband processed image is slightly defocused. When analyzing the results, note that we did observe a lower intensity around 25 kHz, corresponding to a local dip in the receiver array. There is also a strong multipath for the upper part of the LF band, and this could reduce the change in the contrast estimate over the methods.

In Table 1 we also present the estimated contrast on both the HF and the LF images, and these results support our qualitative assessment.

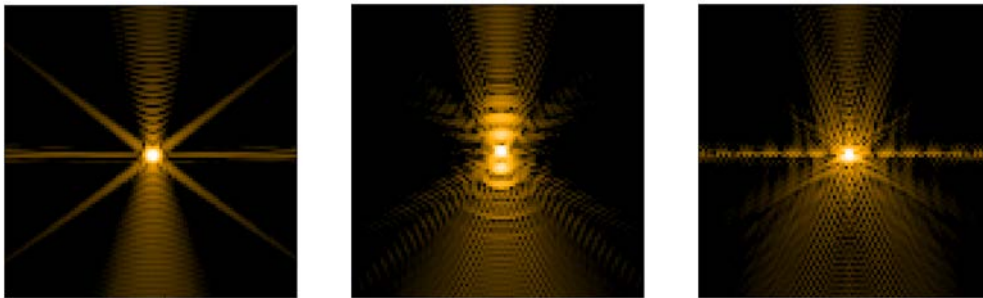


Fig. 6: Narrowband (left), multiband (centre) and wideband (right) point spread functions. The images are $2\text{ m} \times 2\text{ m}$, and the dynamic range shown is 70 dB.

Image processing scheme	Contrast of HF image	Contrast of LF image
Narrowband	6.3	4.3
Multiband	5.9	4.5
Wideband	6.5	5.3

Table 1: Contrast of the HF and LF images processed with the different schemes. The corresponding images are shown in Fig. 7.

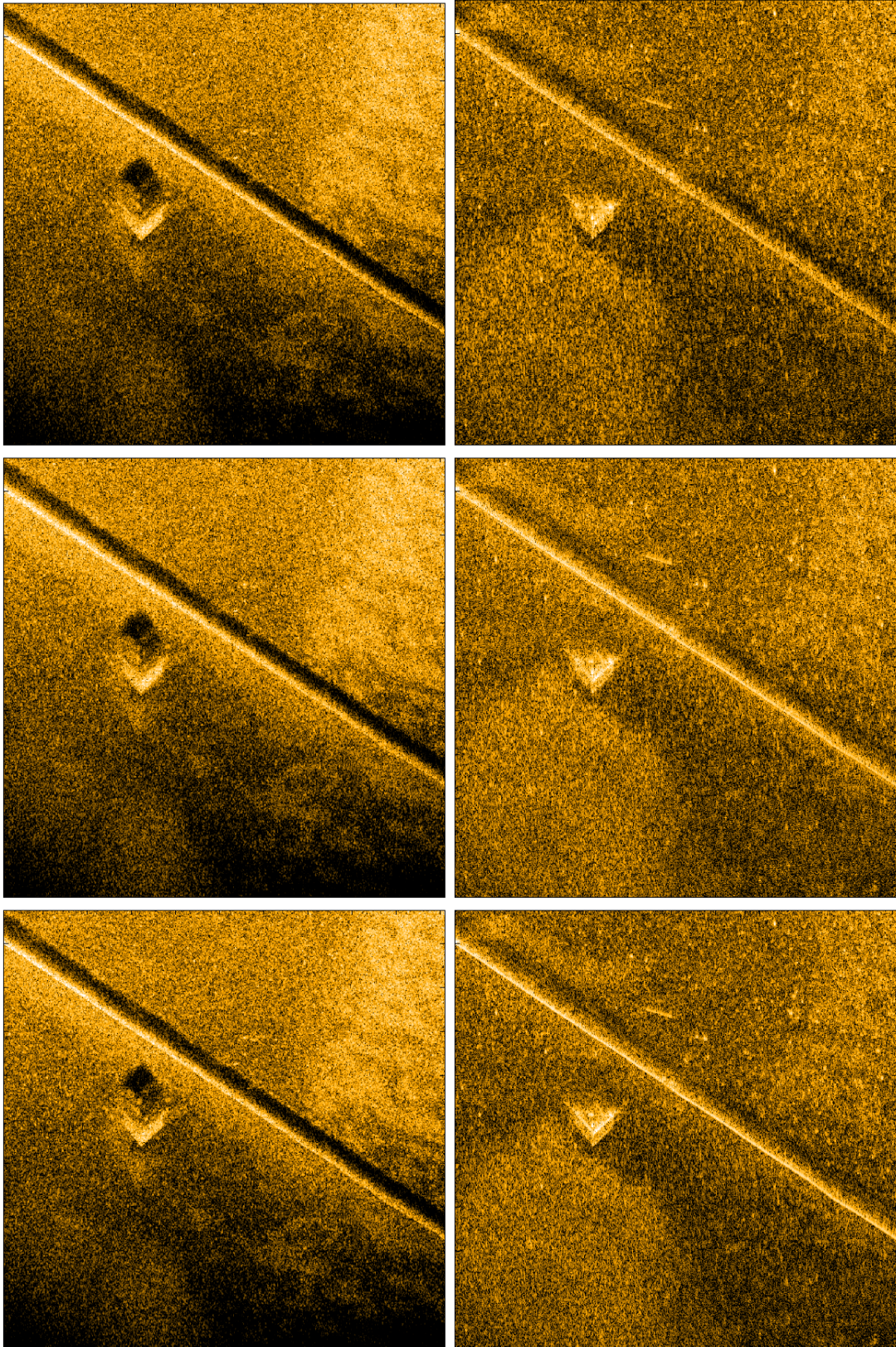


Fig. 7: SAS images from HF 65-80 kHz (left) and LF 12-38 kHz (right) using the three processing schemes; Narrowband processing (top), Multiband processing (centre) and Wideband processing (bottom). All images have been normalized to their maximum value. The images are 20m x 20m. The intensity span [-50, -5] dB for HF and [-45, -5] for LF.

5. CONCLUSION

We have suggested a new wideband SAS imaging method where we adopted the most desired features from both time domain back projection (TDBP) and wavenumber domain (WD) imaging. The new wideband SAS processing scheme has been tested on both recorded data and simulated data from a point scatterer. The method outperforms both the narrowband TDBP and a multiband adaptation for SAS imaging on ultra wideband low frequency (UWB LF) signal, while performing equally well as the narrowband method on high frequency signals.

6. ACKNOWLEDGEMENTS

Thanks to Alan Hunter at TNO for fruitful discussions during the iSAAM meeting in Leesburg, USA, in December 2012. Also thanks to Hayden John Callow at Kongsberg Maritime and Torstein Olsmo Sæbø at FFI for many fruitful discussions.

REFERENCES

- [1] **Williams, K. L., Kargl, S. G., Thorsos, E. I., Burnett, D. S., Lopes, J. L., Zampoli, M., & Marston, P. L.**, Acoustic scattering from a solid aluminum cylinder in contact with a sand sediment: measurements, modeling, and interpretation. *The Journal of the Acoustical Society of America*, 127(6), pp. 3356–3371, 2010.
- [2] **Roy Edgar Hansen**, Introduction to Synthetic Aperture Sonar, In *Sonar Systems*, N. Z. Kolev (Ed.), InTech.: www.intechopen.com/articles/show/title/introduction-to-synthetic-aperture-sonar, 2011.
- [3] **Reigber, A., Alivizatos, E., Potsis, A., & Moreira, A.**, Extended wavenumber-domain synthetic aperture radar focusing with integrated motion compensation, In *IEE Proceedings - Radar, Sonar and Navigation*, pp. 301–310, 2006.
- [4] **Frey, O., Magnard, C., Rüegg, M., & Meier, E.**, Non-linear SAR data processing by time-domain back-projection, In *Synthetic Aperture Radar (EUSAR)*, pp. 1–4, 2008.
- [5] **Goodman, R., Tummala, S., & Carrara, W.**, Issues in ultra-wideband, widebeam SAR image formation, In *Proceedings International Radar Conference*, pp. 479–485, 1995.
- [6] **Chatillon, J., Bouhier, M.-E., & Zakharia, M. E.**, Synthetic aperture sonar for seabed imaging: relative merits of narrow-band and wide-band approached, *IEEE Journal of Oceanic Engineering*, 17(1), pp. 95–105, 1992.
- [7] **Hayes, M. P., & Gough, P. T.**, Broad-band synthetic aperture sonar, *IEEE Journal of Oceanic Engineering*, 17, pp. 80–94, 1992.